

A low LET radiation spectrometer for measuring particle doses in space- and aircraft

E.G. Stassinopoulos¹, C.A. Stauffer², G.J. Brucker³, and Ts.P. Dachev⁴

Abstract

This paper presents experimental data that demonstrates the feasibility of fabricating a miniature nuclear particle dosimeter for monitoring doses in aircraft and satellites. The basic instrument is a Low Linear-Energy-Transfer (LET) Radiation Spectrometer (LoLRS) that is designed to measure the energy deposited by particles with low LET values. The heart of the instrument is a Silicon-Lithium Drifted Diode (SLDD). Test results show that the LoLRS can be used to monitor the radiation threat to personnel in flights of space- and aircraft and also to generate a comprehensive data base from aviation and satellite measurements that can contribute to the formulation of more accurate environmental radiation models for dose predictions with reduced uncertainty factors.

1. 0 Introduction and background

Particles with low LET values expose the crews of commercial aircrafts or space vehicles, such as the Shuttle or Space Station, to total doses that pose a threat to their health. Crews working on present-day aircraft are estimated to receive one of the highest average equivalent-doses of any group of workers in the United States. Crews of future commercial aircraft, flying at greater elevations, will be exposed to even higher doses. Present calculations of such exposures are uncertain because knowledge of important components of the radiation field comes from theoretical predictions. Currently the highest exposures are experienced by crews flying over the polar regions and on the supersonic CONCORDE planes. Crews on flights that occur during a solar event can be exposed to larger than normal doses, particularly when the flights are at high altitudes.

The instrument evolved from an international cooperative project by a group of Bulgarian, and American scientists [1,2,3]. The spectrometer is a compact, low power, lightweight instrument with a SLDD detector and supporting electronics that enable it to operate as a pulse height analyzer of energy deposited in the device by energetic particles. Tissue dose or dose rate can be deduced from the measurements on the basis of calibration results.

2.0 Description of LoLRS

The basic detector of radiation in the LoLRS is a lithium-drifted silicon diode, 1 mm thick and fully depleted, with a sensitive area of 1 cm² and a weight of 0.232g. Figure 1 contains a block diagram that shows the supporting electronics. The nuclear-reaction particles that are incident on the diode produce pulses of charge that are passed to the charge sensitive amplifier and then to the discriminator and peak hold detector. Finally, they are converted from analog to digital signals by the 8-bit Analog-to-Digital Converter (ADC) and sorted into 256 channels according to their voltage amplitudes. Two microprocessor units manage the data flow to and out of the flash memory devices. The specifications and dynamic ranges of the instrument are listed in Table 1. The energy deposited (or loss) in the silicon diode by the incident particles ranges from 0.16 to 13.8 MeV. The instrument's measurement-time-per-spectrum can be varied from 30 seconds to 30 minutes.

1. NASA Goddard Space Flight Center, Greenbelt, MD, 20771 USA
2. Stinger Ghaffarian Technologies, MD, 20771 USA
3. REC, Inc., West Long Branch, NJ, 07764 USA
4. Bulgarian Academy of Sciences, Solar Terrestrial Influences Laboratory, Sofia, Bulgaria

The LoLRS operates in two modes, namely the “Data Collecting Mode” and the “Data Transfer Mode”. In the “Data Collecting Mode”, the instrument is connected via a jack to a polarized relay. In this mode the device is operating under the control of the program in the microprocessors to collect dose, flux, and spectra until the memory is filled. At that time, the instrument is automatically turned off through the relay. The total time the monitor can spend in the “Data Collecting Mode” depends on the number of batteries attached to the instrument. Usually it is about 480 to 720 hours. In the “Data Transfer Mode” the device allows the transfer of the data accumulated in the flash memory to a personal computer (PC) under a parallel port communication link. During this mode the data are correlated to the real time of the flight.

The major parameter of the instrument is the amplitude of the charge pulses generated in the solid state detector (SSD) by the incident particles. Those pulses are then passed to the charge-sensitive amplifier that converts them to corresponding voltage pulses. These signals are subsequently amplified by a factor of 5 in the main amplifier stage. The sensitivity or conversion factor of this pre-amplifier is 240 mV/MeV. The threshold setting of the discriminator is 51.6 mV which establishes the lower data limit and consequently, the number of channels assigned to instrument background signals. Since there are 256 channels in the Analog-to-Digital converter and the upper voltage limit is 3.3 V, the sensitivity per channel is $3.3/256 = 12.89$ mV/Ch and thus the first four channels are assigned to storing the background pulses. The remaining channels are assigned to storing pulses caused by the neutron-induced secondary particles. The deposited energy (Dep E) is given by equation :

$$\text{Dep E(MeV)} = \sum_{i=4-256} (\text{counts}_i * \text{channel}_i) * M \quad (1)$$

where the conversion factor M is given by:

$$M = \left(12.89 \frac{mV}{Ch} \right) / \left(240 \frac{mV}{MeV} \right) = 0.05371 \frac{MeV}{Ch} \quad (2)$$

and the corresponding dose rate, D_R by:

$$D_R (\mu\text{Gy}_{si}/h) = K * \text{Dep E (MeV)} / t_c \quad (3)$$

where t_c is the collection time (in seconds), h is normalized time in hours, and the conversion factor K is: $K = 2.486$, in units of $\mu\text{Gy}_{si} * s / h - \text{MeV}$.

3.0 Characterization tests of LoLRS

The instrument was subjected to thermal tests by the thermal testing group at the Goddard Space Flight Center. The thermal profile was as follows: 0° to -40°C at a rate of $\pm 2^\circ\text{C}$ per 5-minute intervals for a duration at extreme level of 2 hours. Throughout this test, the LoLRS performed flawlessly.

The spectrometer can detect and measure tissue doses produced by cosmic ray progeny such as neutrons, protons, and other types of interaction particles. In aircraft, the major contributors to the total dose are protons and neutrons. The dose produced by neutrons is not directly due to the incident neutrons but is due to the products from neutron interactions in the silicon diode (SLDD) and the surrounding materials. Tests to characterize the instrument’s sensitivity to some of those particle environments were conducted at the Indiana University, Bloomington cyclotron facility. The LoLRS instrument was exposed to protons ranging in energy from 33.16 to 195 MeV. Figure 2 shows a plot of the average dose per proton

versus the proton energy. The doses are the sum of all the contributions from the 252 data collecting channels, that is, the integral dose normalized by the proton fluence.

4.0 Test Results

All test data presented here were collected on commercial flights during every five minutes of the flight but the conditions of the measurements were not systematically controlled, particularly in terms of location and altitude. Several test flights were conducted in different aircraft and over diverse, short and long routes to evaluate the performance of the instrument in a variety of carriers and conditions. Figure 3 is a plot of dose rate versus time after the instrument was turned on for a flight from Los Angeles to Auckland, New Zealand. Figures 4 and 5 represent plots of measurements for flights from Washington, DC to Denver, CO and then Denver back to Washington the same day, respectively. Figure 6 shows the results for a flight from Paris, France to Washington, DC and Figure 6 shows the test data for flights from Budapest, Hungary to Frankfurt, Germany to Washington, DC.

In most of the commercial flights, altitude information was made available by the airlines after the flights; however, for the trip from Sofia, Bulgaria, to New York, NY altitude data were provided to members of the LoLRS team on-board the plane by the pilot on three occasions, while on a recent flight from Washington, DC, to Frankfurt, Germany, to Budapest, Hungary, flight information (latitude, longitude, altitude, speed, temperature) was continuously presented on TV monitors in the cabin. It should be noted, however, that for some flights altitude data could not be obtained. Table 2 lists the total and average doses measured for test flights between the indicated cities.

5.0 Discussion

It is well established that cosmic rays of galactic and solar origin interact with the constituents of the Earth's atmosphere, creating cascades of secondary energetic particles, of which neutrons and protons are the most numerous and damaging components. A great deal of study, both theoretical [4] and experimental [5] has been devoted to defining the radiation field that is established at aviation altitudes by these secondary particles.

For all flights reported in Figures 3 to 7, the peak dose rates are a function of two variables: altitude and magnetic latitude. Thus, in Figure 3 for the trip from Los Angeles to Auckland, the dose rate remained around $0.07 \mu\text{Gy}/5\text{-min}$ for the major part of the flight over the Pacific Ocean, and only climbed to a peak of about $0.12 \mu\text{Gy}/5\text{-min}$ near the end of the trip (last 2.5 hours). The peak rate during the flight covered in Figure 4, Washington to Denver, was about $0.14 \mu\text{Gy}/5\text{-min}$. However, the peak rate achieved a surprisingly high level of $0.28 \mu\text{Gy}/5\text{-min}$ for the Denver to Washington flight, as shown in Figure 5.

Figures 6 and 7 show data for test flights from Paris, France, and one from Frankfurt, Germany, to Washington, DC respectively. The flight from Paris to Washington indicates a constant rise in rate with a peak of about $0.23 \mu\text{Gy}/5\text{-min}$ at the end of the trip. A similar constant increase in rate can be seen in the plot of dose rate in Figure 7 for the Frankfurt to Washington flight and about the same peak rate of $0.23 \mu\text{Gy}/5\text{-min}$. The steady increases are due to the increase in altitude as the flights progressed towards Washington.

All flights indicate background levels on the ground before take-off and after landing that range from 0.017 to $0.033 \mu\text{Gy}/5\text{-min}$. However, upon close examination it is apparent that the data from low altitude locations like Washington, Houston, and Los Angeles, with elevations less than 100 feet above sea level, have almost the same values as data from elevated locations as, for example, Snowmass, CO at over

9000 feet altitude; that is, an average of about 0.0208 $\mu\text{Gy}/5\text{-min}$ and 0.0225 $\mu\text{Gy}/5\text{-min}$, respectively. We should have observed a much larger difference at these two altitudes. The normal global average rate of radiation background levels, excluding high concentrations of naturally occurring radionuclides such as radium, thorium, uranium, etc., has been reported to be about 0.008 to 0.017 $\mu\text{Gy}/5\text{-min}$ at about 1 meter above ground and including cosmic ray contributions coming from above [6]. It has been established that the detector orientation has no discernible effect on the measurements, in flight or on the ground. On the basis of these test results, we conclude that the LoLRS instrument has a relatively elevated background level. This affects the resolution in the lowest channels and limits the use of the instrument to elevations above 9000 ft.

An example of an application of the LoLRS is shown in Table 2, where the total accumulated dose for each flight, the flight duration in minutes, and the average dose-rate per minute are presented. The highest exposure occurred on the Denver, CO to Washington, DC trip (3.84×10^{-2} $\mu\text{Gy}/\text{min}$) and the lowest on the Auckland, N.Z. to Christchurch, N.Z. segment (1.10×10^{-2} $\mu\text{Gy}/\text{min}$), a factor of about 3.5 different. Other high doses were experienced on the Washington-Paris/Paris-Washington and the Washington-Frankfurt/Frankfurt-Washington flights. This is probably due to the fact that all of these flights traveled some of their time at high magnetic latitudes.

6.0 Conclusions

Test flights have shown the LoLRS instrument to be an effective and reliable radiation monitor for aviation or space applications. It is characterized by small size, low power, lightweight, and low cost. The instrument is currently being deployed on demonstration-test flights for global surveys of radiation environment levels within aircraft and on high-altitude balloon missions over the south pole (U.S. Antarctic Program) and will next be used in scientific research missions.

7.0 Acknowledgement

Airport, for his valuable help in providing us with important altitude data for some past flights. The authors wish to express their appreciation to UNITED AIRLINES for assisting in this research, with special thanks to Rick Koski, UNITED's shift manager at Washington's Dulles International Airport, for his valuable help in providing us with important altitude data for some past flights.

8.0 References

- [1] Ts. P. Dachev, J. Semkova, V. Petrov, V. Redko, V. Bengin, T. Kostereva, J. Miller, L. Heilbronn, C. Zeitlin, "Analysis of the Pre-flight and Post-flight Calibration Procedures Performed on the LIULIN Space Radiation Dosimeter", *Acta Astronautica*, 42, 375, 1998.
- [2] Ts. P. Dachev, J. V. Semkova, Ju. N. Matvichuk, B.T. Tomov, R.T. Koleva, P.T. Baynov, V.M. Petrov, V.M. Shurshakov, Yu. Ivanov, "Inner Magnetosphere Variations After Solar Proton Events. Observations on Mir Space Station in 1989-1994 Time Period", *Adv. Space Res.*, 22, No 4, 521, 1998.
- [3] Ts. P. Dachev, B.T. Tomov, G. Georgiev, P.G. Dimitrov, Yu. N. Matviichuk, V.M. Petrov, V.V. Shurshakov, E.G. Stassinopoulos, and J. Bart, "Analysis of the Calibration Results of the Engineering Model of LIULIN-3 Radiometer-Dosimeter", *Proceedings of the 3rd National Conference on Solar-Terrestrial Influences, II-73, Sofia, Bulgaria, June 1998. (In Bulgaria)*

- [4] E. Normand, Single-Event effects in avionics, IEEE Trans. on Nucl Sci., vol. 43, No. 2, April, 1996.
- [5] C. S. Dyer, A. Sims, and C. Underwood, Measurements of the SEE environment from sea level to GEO using the CREAM and CREDO experiments, IEEE Trans. on Nucl. Sci., vol. 43, No. 2, April, 1996.
- [6] P.F. Gustafson and S.S. Brar, Gamma-Emitting radionuclides in soil, The Natural Radiation Environment, Editors John A.S. Adams and Wayne H. Lowder, University of Chicago Press, 1964.

Figure Captions

1. Block diagram of LoLRS electronic setup.
2. Characterization of LoLRS' sensitivity to protons. Plot shows the tissue dose per proton measured by the LoLRS instrument versus proton energy..
3. LoLRS test flight data, dose rate versus minutes after turn-on of instrument, Los Angeles, CA to Auckland, NZ (12/8/97).
4. LoLRS test flight data dose rate versus minutes after turn-on of instrument, Washington, DC to Denver, CO.
5. LoLRS test flight data, dose rate versus minutes after turn-on of instrument, Denver, CO to Washington, DC
6. LoLRS test flight data, dose rate versus minutes after turn-on of instrument, Paris, France to Washington, DC. (9/22/97)
7. LoLRS test flight data, dose rate versus minutes after turn-on of instrument, Budapest, Hungary to Frankfurt, Germany to Washington, DC. (3/30/98).

Table Captions

1. LoLRS specifications and dynamic ranges.
2. Sample data of total doses, average dose rates, and flight durations.

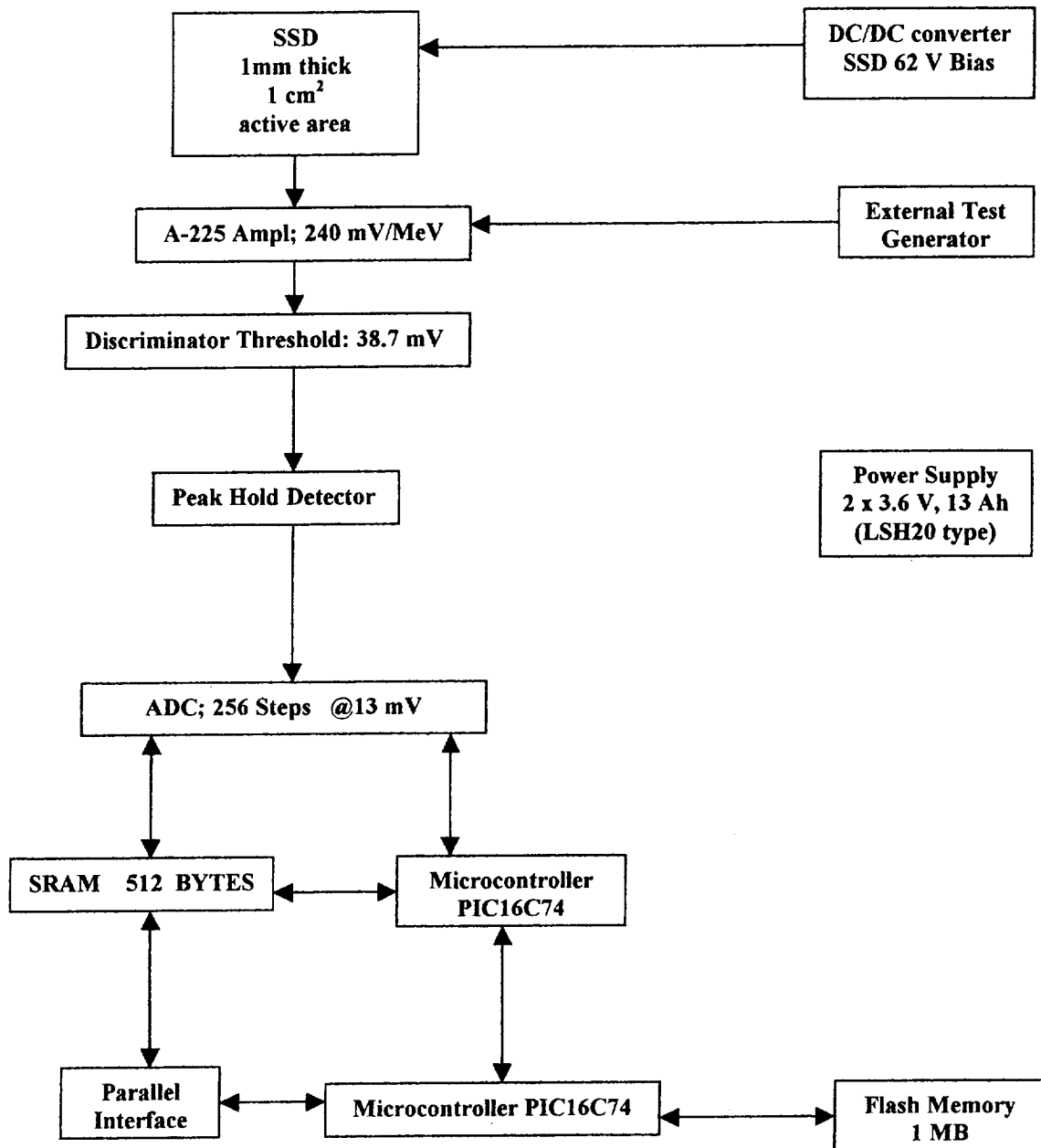
TABLE I

<u>Specifications</u>	<u>Ranges</u>
Mass: (including batteries) 960 g	Flux: 1 – 5000 part/cm ² -s
Size: 140 x 80 x 30 mm ³	Energy Deposited: 0.16 – 13.8 MeV
Temperature: -20°C to +45°C	LET: 0.16-13.8 keV/μ (silicon)
Measurement Time: 30s to 30 min	(6.88-593) x 10 ⁻⁴ MeV-cm ² / mg

TABLE II

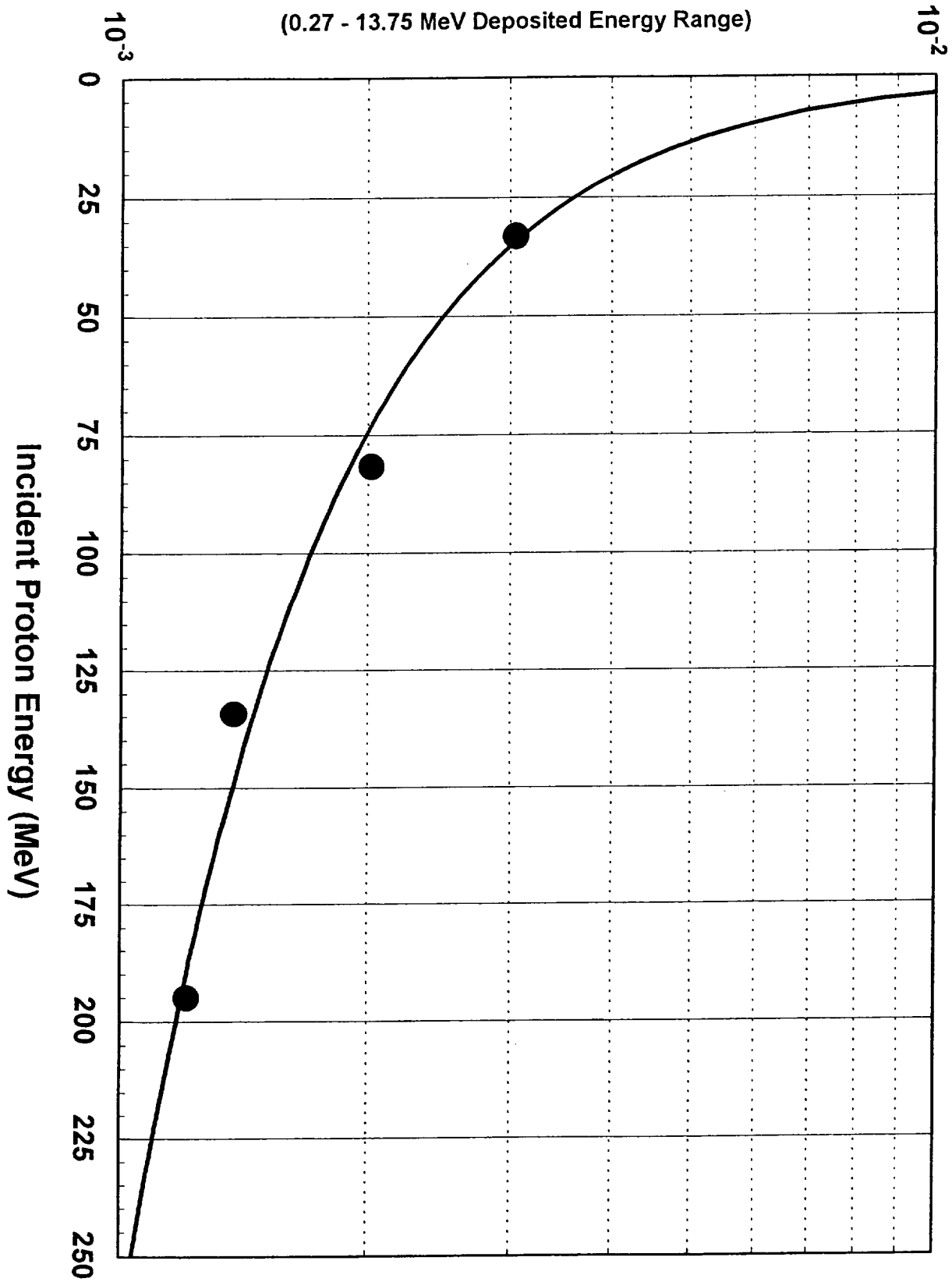
Departure Airport	Arrival Airport	Figure	Total Flight Dose (μGy)	Flight Duration (minutes)	Average Dose ($\mu\text{Gy}/\text{min} \times 10^{-2}$)
Washington, DC	Los Angeles, CA	x	7.073	260	2.72
Los Angeles, CA	Auckland, NZealand	2	10.483	685	1.53
Auckland, NZealand	Christchurch, NZealand	x	0.604	55	1.10
Washington, DC	Denver, CO	3	3.967	185	2.14
Denver, CO	Houston, TX	x	1.773	90	1.97
Houston, TX	Denver, CO	x	2.512	95	2.64
Denver, CO	Washington, DC	4	5.187	135	3.84
Washington, DC	Paris, France	x	12.018	380	3.16
Paris, France	Washington, DC	5	14.835	435	3.41
Sofia, Bulgaria	New York, NY	x	16.387	555	2.95
Washington, DC	Frankfurt, Germany	x	12.739	390	3.27
Frankfurt, Germany	Budapest, Hungary	x	1.236	60	2.06
Budapest, Hungary	Frankfurt, Germany	x	1.219	60	2.03
Frankfurt, Germany	Washington, DC	6	14.721	460	3.20

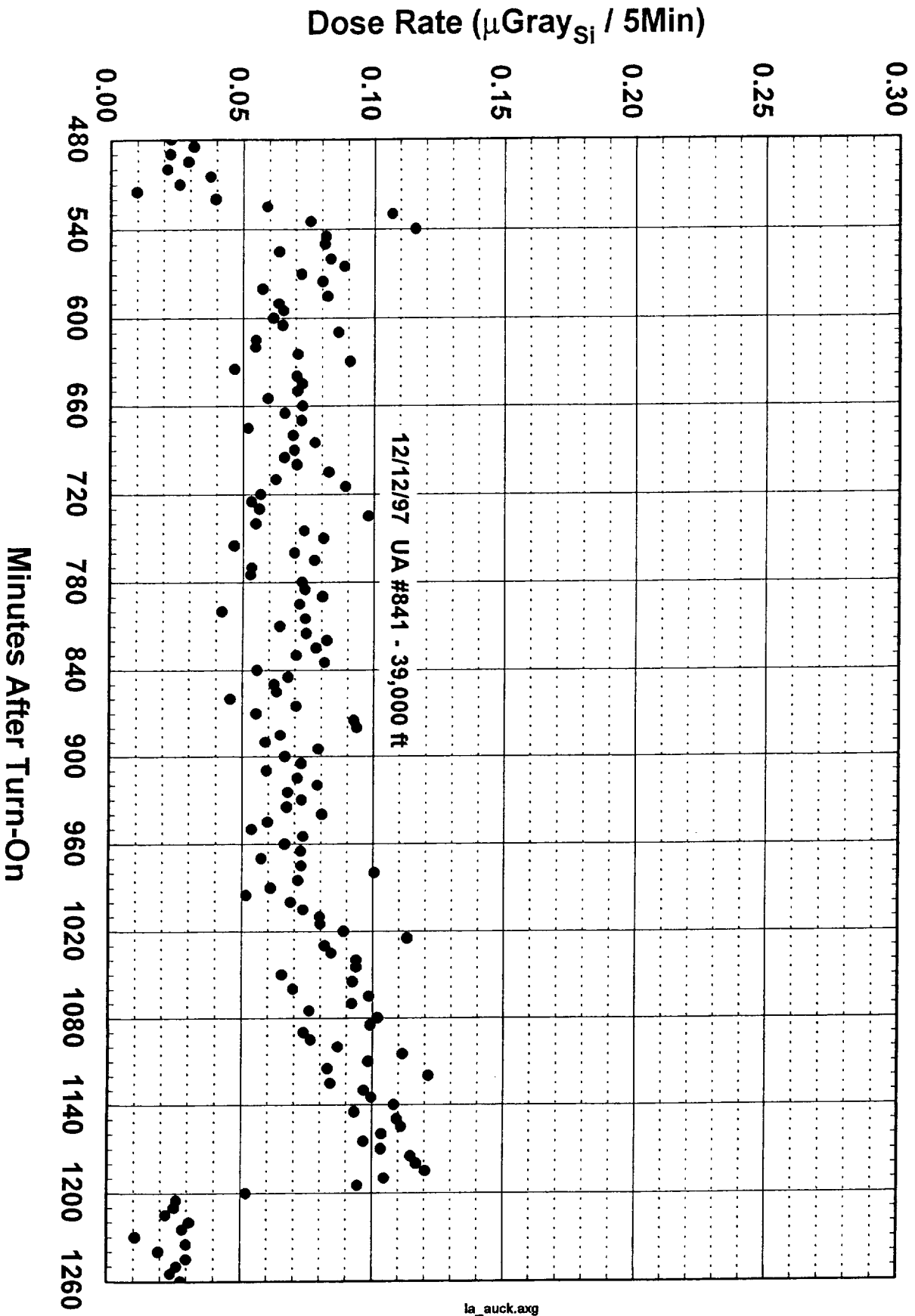
FIGURE I

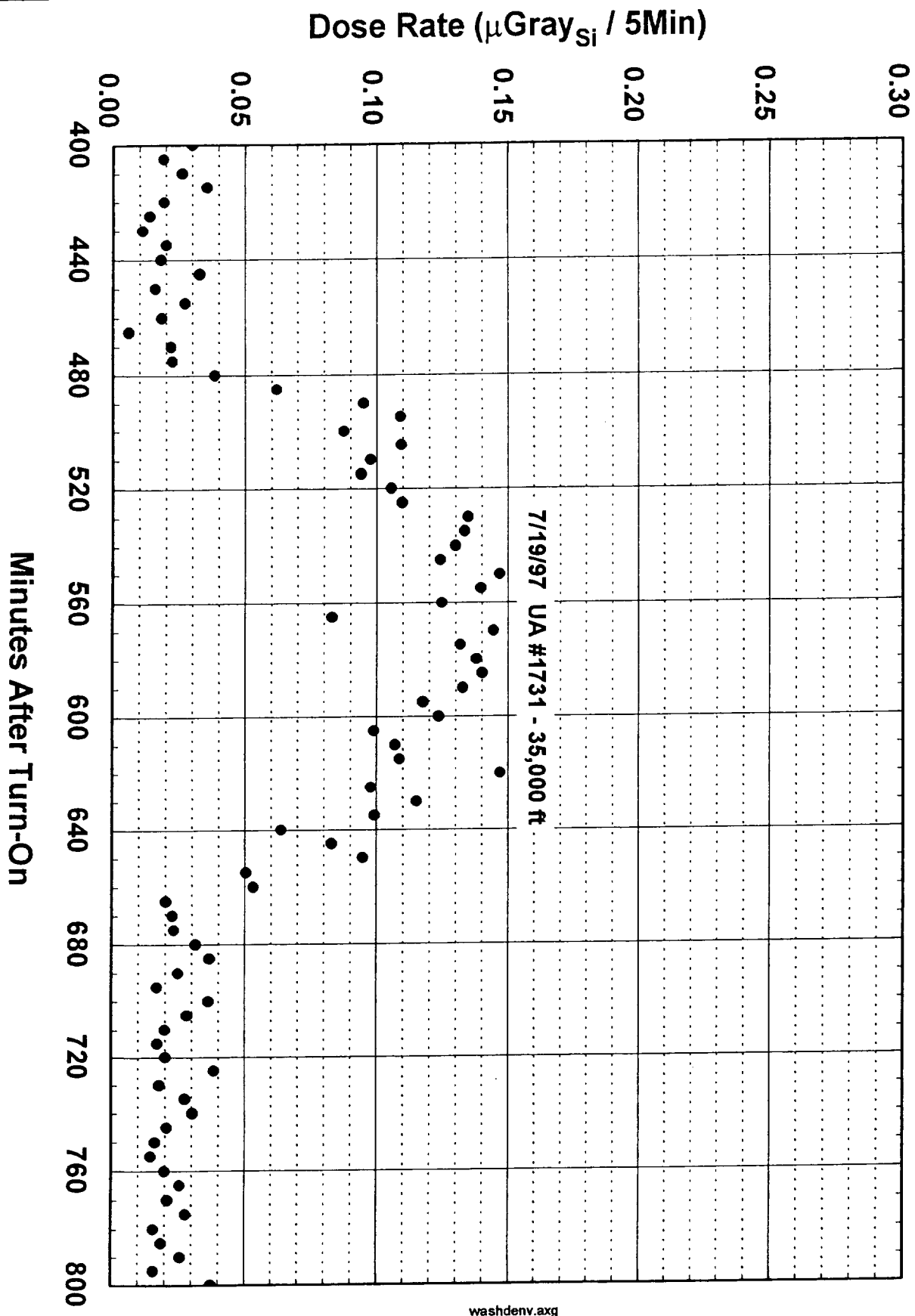


Average Dose ($\mu\text{Gray}_{\text{Si}}$) Per Proton

(0.27 - 13.75 MeV Deposited Energy Range)







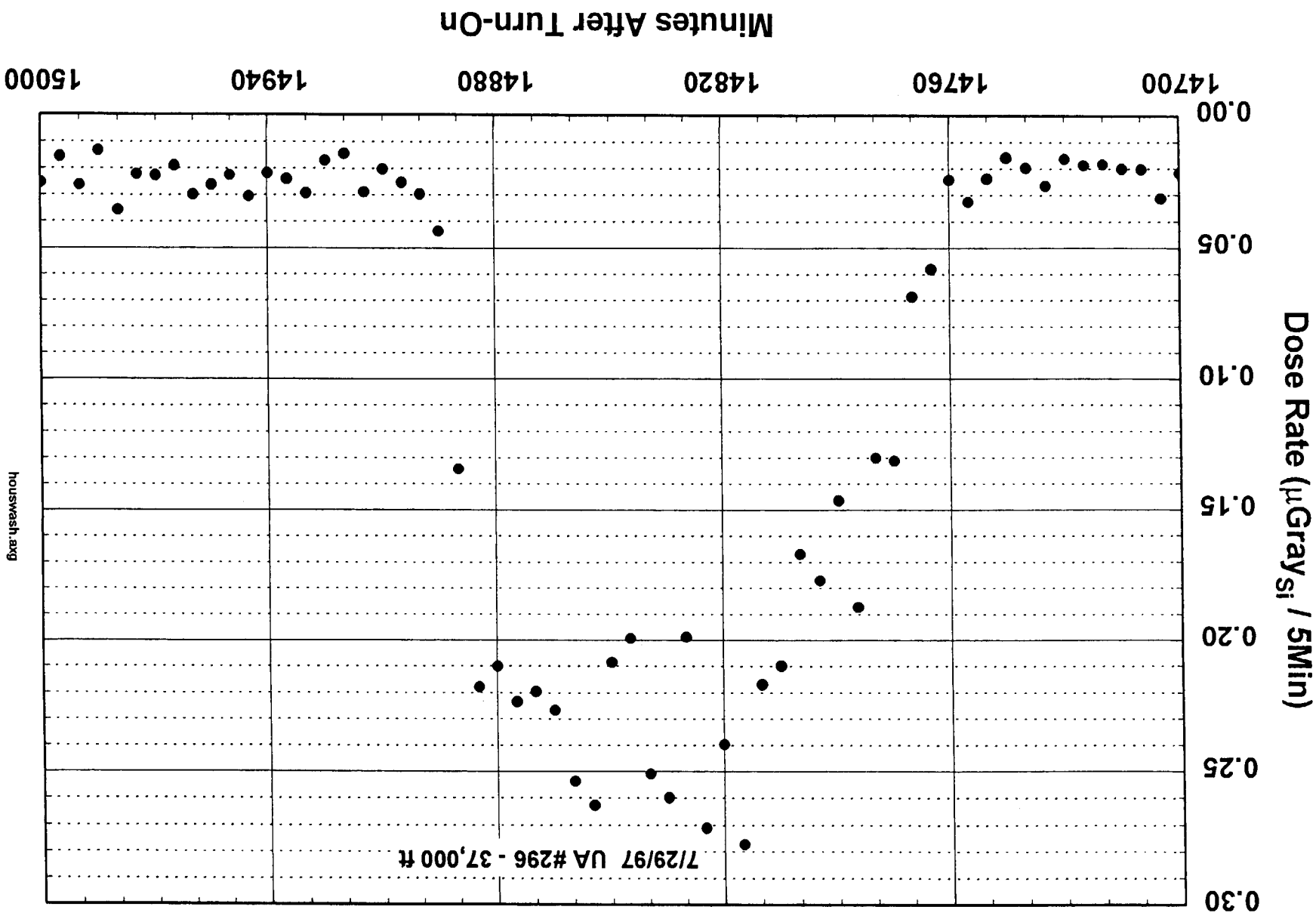


FIGURE V

